

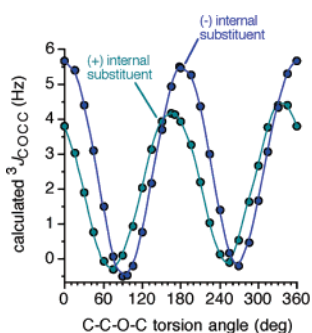
## Oligosaccharide Trans-Glycoside $^3J_{\text{COCC}}$ Karplus Curves Are Not Equivalent: Effect of Internal Electronegative Substituents

Hongqiu Zhao,<sup>†</sup> Ian Carmichael,<sup>‡</sup> and Anthony S. Serianni<sup>\*†</sup>

Department of Chemistry and Biochemistry and the  
Radiation Laboratory, University of Notre Dame,  
Notre Dame, Indiana 46556-5670

aseriann@nd.edu

Received October 23, 2007



Phase shifting of  $^3J_{\text{COCC}}$  Karplus curves for C-O-C-C coupling pathways bearing an internal electronegative substituent.

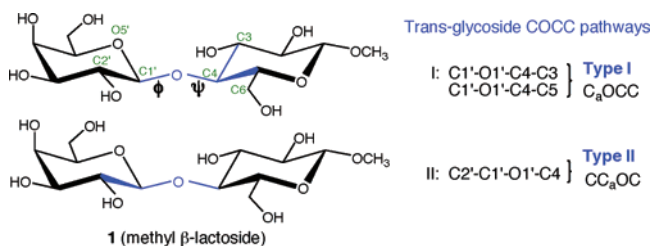
Density functional theory (DFT) calculations show that internal electronegative substituents perturb  $^3J_{\text{COCC}}$  Karplus curves by phase shifting them with respect to analogous pathways devoid of this substitution. Thus, the  $J$ -coupling maximum, which normally is observed near  $180^\circ$ , is shifted by  $\sim 15^\circ$ . These findings suggest that the two types of inter-residue C-O-C-C coupling pathways observed in many oligosaccharides cannot be treated using a generalized  $^3J_{\text{COCC}}$  Karplus equation. Quantitative interpretations of trans-glycoside  $J$ -couplings to evaluate linkage conformations will need to take this effect into account.

Trans-glycoside (inter-residue) NMR  $^3J_{\text{COCC}}$  spin-spin coupling constants have attracted increased attention in recent years as experimental parameters to improve the assignment of linkage conformation of oligosaccharides in solution.<sup>1,2</sup> These couplings show the expected primary Karplus dependence on the central C-O bond torsion, but secondary structural factors also influence them. An example of the latter is the effect of terminal electronegative substituents, with in-plane oxygens on either of the terminal (coupled) carbons increasing the observed coupling by  $\sim 0.7$  Hz.<sup>1</sup> As part of efforts to characterize these secondary dependencies, we posed the following question: Are the two types of inter-residue C-O-C-C coupling pathways present

in oligosaccharides equivalent, that is, can both be treated adequately using a single, generalized Karplus equation that accounts for the effects of terminal in-plane oxygen? We show herein that these pathways are nonequivalent and should be treated using separate parametrized equations.

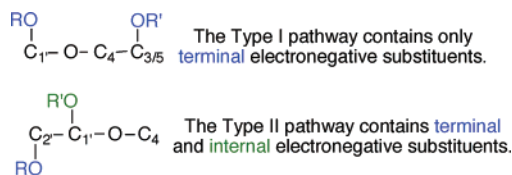
Two different trans-glycoside C-O-C-C coupling pathways are present in oligosaccharides, as illustrated using methyl  $\beta$ -lactoside **1** (Scheme 1). Type I involves C1' as a terminal

### SCHEME 1



coupled carbon, is denoted a C<sub>a</sub>OCC pathway, where C<sub>a</sub> is an anomeric carbon, and is sensitive to the O1'-C4 bond torsion ( $\psi$ ). Type II involves C2' as a terminal coupled carbon, is denoted a CC<sub>a</sub>OC pathway, and is sensitive to the C1'-O1' bond torsion ( $\phi$ ). A generalized representation of both pathways (Scheme 2) illustrates that the C<sub>a</sub>OCC pathway contains two

### SCHEME 2



terminal and no internal electronegative substituents, whereas the CC<sub>a</sub>OC pathway contains one terminal and one internal electronegative substituent. At issue is whether the internal substituent perturbs the coupling behavior.

Earlier work on  $^3J_{\text{COCC}}$  parametrization for  $O$ -glycosidic linkages hinted at different behaviors for Type I and Type II pathways. Using  $\beta$ -(1 $\rightarrow$ 4)-linked disaccharide mimics,  $^3J_{\text{C1',C3}}$ ,  $^3J_{\text{C1',C5}}$ , and  $^3J_{\text{C2',C4}}$  values were calculated by density functional theory (DFT) as a function of the central torsion angle (Figure S1, Supporting Information).<sup>2</sup> Noteworthy was an apparent shift of the maximal  $^3J_{\text{C2',C4}}$  value from the expected C2'-C1'-O1'-C4 torsion angle of  $180^\circ$ . However, because structures were confined to those having an optimal exoanomeric effect, and data collection was confined to only one-half of the full  $360^\circ$  torsional range, firm conclusions about the significance of this shift could not be made.

$^3J_{\text{COCC}}$  values were calculated by DFT as a function of the central bond torsion for the Type I and Type II coupling pathways in structures **2a** and **2b**, respectively (Figure 1A). The overall shape of the two curves is conserved, but two differences are noteworthy: curve amplitude is slightly reduced for the Type II pathway in **2b**, and more importantly, the curve is phase shifted to the left, yielding a coupling maximum at  $\sim 165^\circ$  compared to  $180^\circ$  for the Type I pathway in **2a**.

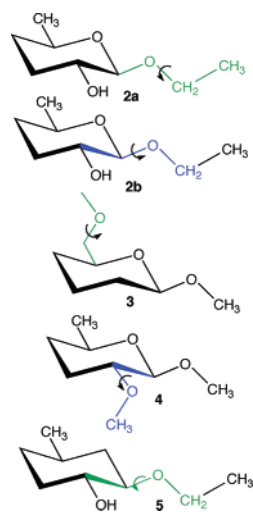
Coupling pathways in **3** and **4** were also investigated. The C-O-C-C pathway in **3** involves an exocyclic primary

<sup>†</sup> Department of Chemistry and Biochemistry.

<sup>‡</sup> Radiation Laboratory.

(1) Bose, B.; Zhao, S.; Stenutz, R.; Cloran, F.; Bondo, P. B.; Bondo, G.; Hertz, B.; Carmichael, I.; Serianni, A. S. *J. Am. Chem. Soc.* **1998**, *120*, 11158–11173.

(2) (a) Cloran, F.; Carmichael, I.; Serianni, A. S. *J. Am. Chem. Soc.* **1999**, *121*, 9843–9851. (b) Olsson, U.; Serianni, A. S.; Stenutz, R. *J. Phys. Chem.* **2008**, in press.

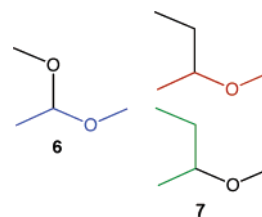


alcoholic carbon, whereas that in **4** corresponds to an alternate Type I pathway. Neither pathway contains an internal electronegative substituent, and both curves show a coupling maximum at  $\sim 180^\circ$  (Figure 1B). Curve amplitude is slightly greater for **3** than for **4**.

A comparison was then made between the C–O–C–C coupling pathways in structures **2b** and **5**. Note that both pathways are identical except that, in **5**, the ring oxygen is absent and thus the pathway lacks an internal electronegative substituent. The curve for **5** displays a maximum at  $\sim 180^\circ$  (Figure 2A), as observed for **2a**, **3**, and **4** (Figure 1), lending further support to the contention that internal electronegative substituents are responsible for the phase shifting.

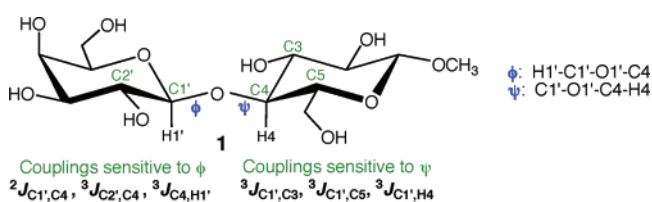
The generality of this substituent effect was tested in simplified structures **6** and **7**. The blue pathway in **6** contains

an internal electronegative substituent. In **7**, a C–C–C–C pathway containing an internal electronegative substituent (green pathway) and a C–O–C–C pathway devoid of this internal substitution (red pathway) are present. Calculated Karplus curves (Figure 2B) show that only the C–O–C–C pathway in **7** gives a maximum coupling at  $180^\circ$ . These results show that the internal electronegative substituent effect exists in both C–O–C–C and C–C–C–C coupling pathways.



These findings have important implications for the interpretation of trans-glycoside  $^3J_{\text{COCC}}$  values in oligosaccharides. Three trans-glycoside  $J$ -couplings in **1** (Scheme 3) depend on the  $\phi$

### SCHEME 3



torsion:  $^2J_{\text{C1}',\text{C4}}$ ,  $^3J_{\text{C4},\text{H1}'}$ , and  $^3J_{\text{C2}',\text{C4}}$ . The geminal  $^2J_{\text{C1}',\text{C4}}$ , has limited dynamic range and is mainly affected by  $\phi$  but also by other structural parameters, such as the C1'–O1'–C4 bond angle.<sup>3</sup> The vicinal  $^3J_{\text{C4},\text{H1}'}$  displays a Karplus curve symmetric about the H1'–C1'–O1'–C4 torsion angle of  $0^\circ$ , and its interpretation is problematic when discrimination between single and multiple state conformational models is required. Thus, the remaining vicinal  $^3J_{\text{C2}',\text{C4}}$  bears significant weight in the assignment of linkage conformation about  $\phi$ . The present results show that coupling behavior for this  $\text{CC}_a\text{OC}$  pathway is anomalous in that maximal couplings cannot be expected when the coupled carbons are anti. This difference, in addition to an apparent slight decrease in the amplitude of  $\text{CC}_a\text{OC}$  curves relative to  $\text{C}_a\text{OCC}$  curves, must be taken into account in quantitative studies.

The underlying cause of the phase shift in Karplus curves for internally substituted C–O–C–C pathways is beyond the scope of the present discussion. However, inspection of Karplus curves calculated for  $^3J_{\text{C2}',\text{C4}}$  in **1** shows that the two gauche couplings are nonequivalent. Gauche rotamer **II** (C2'–C1'–O1'–C4 pathway) yields a smaller  $^3J_{\text{C2}',\text{C4}}$  ( $\sim 0$  Hz) than does gauche rotamer **III** ( $\sim 1.5$  Hz) (Scheme 4, Figure S2, Supporting

### SCHEME 4

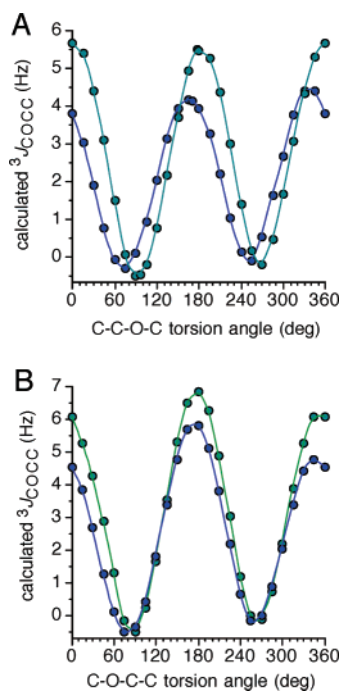
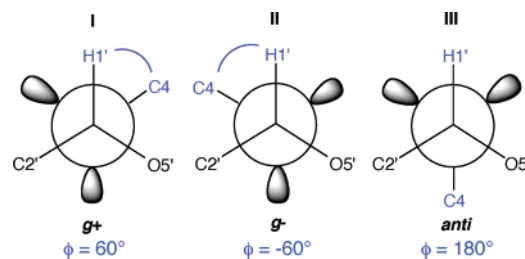


**FIGURE 1.** (A) Calculated  $^3J_{\text{COCC}}$  values in **2a** (green symbols) and **2b** (blue symbols) as a function of the central C–O bond torsion. Pertinent coupling pathways are highlighted in green in **2a** and blue in **2b**. (B) Calculated  $^3J_{\text{COCC}}$  values in **3** (green symbols) and **4** (blue symbols) as a function of the central C–O bond torsion. Pertinent coupling pathways are highlighted in green in **3** and blue in **4**.

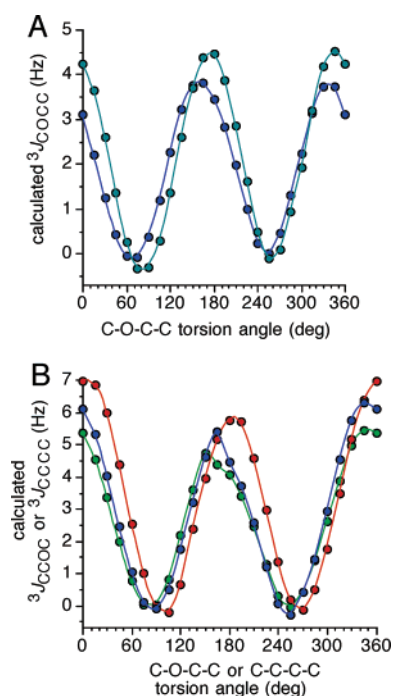


**FIGURE 2.** (A) Calculated  $^3J_{\text{COCC}}$  values in **2b** (blue symbols) and **5** (green symbols) as a function of the central C–O bond torsion. Pertinent coupling pathways are highlighted in blue in **2b** and green in **5**. (B) Calculated  $^3J_{\text{COCC}}$  values in **6** (blue symbols) and **7** (green symbols for  $^3J_{\text{CCC}}$  and red symbols for  $^3J_{\text{COCC}}$ ) as a function of the central C–O or C–C bond torsion. Pertinent coupling pathways are highlighted in blue in **6** and green in **7**.

Information). This behavior is attributed to the different orientations of O5' with respect to the coupled carbons, being anti to C4 in **II** and gauche to C4 in **III**. By analogy to the behavior of  $^3J_{\text{HH}}$  couplings,<sup>4,5</sup> the anti arrangement is expected to reduce the value of  $^3J_{\text{C2',C4}}$ . This reduction induces asymmetry in the Karplus curve and may be partly responsible for the observed phase shift. However, the shifting is not solely the result of fitting an asymmetric curve. DFT calculations show that maximal coupling is observed at torsions displaced by  $\sim 15^\circ$

(3) Cloran, F.; Carmichael, I.; Serianni, A. S. *J. Am. Chem. Soc.* **2000**, *122*, 396–397.

(4) Günther, H. *NMR Spectroscopy*; Wiley: New York, 1995; pp 119–120.

(5) Pachler, K. G. R. *Tetrahedron* **1971**, *27*, 187–199.

from  $180^\circ$ , and thus the effect appears to be intrinsic and related to that reported for  $^3J_{\text{HCH}}$  Karplus curves for fluoroethane.<sup>4,5</sup>

In conclusion, we have shown that the two types of C–O–C–C coupling pathways across *O*-glycosidic linkages of oligosaccharides are not equivalent and that internal electronegative substituents cause phase shifting of the corresponding Karplus curves. This behavior will be examined in greater detail in forthcoming reports.

## Calculations Section

**DFT Calculations.** Model structures **2–4** contain C–O–C–C coupling pathways that mimic those that exist across *O*-glycosidic linkages of oligosaccharides. Model compounds **5–7** served as structural analogs of **2**. Density functional theory (DFT) calculations using the B3LYP functional<sup>6</sup> and 6-31G\* basis set<sup>7</sup> were conducted within *Gaussian03*<sup>8</sup> for geometric optimization of molecular structures. *J*-Couplings were calculated by DFT within *Gaussian03* using an extended basis set ([5s2p1d|3s1p]).<sup>9</sup> Errors in the calculated couplings are estimated at  $\pm 0.2$ – $0.4$  Hz (absolute error), whereas relative changes in couplings are expected to be more accurate. Different C–O–C–C torsion angles, denoted by color in the structures, were varied from 0 to  $360^\circ$  in  $15^\circ$  increments by holding the angles at fixed values while optimizing all other parameters. Geometry optimizations of all model structures were initiated from reasonably low energy conformations except for the fixed torsion angles indicated above. For example, the C2'–C1'–O1'–CH<sub>3</sub> torsion angles in **3** and **4** started from an anti geometry and remained approximately anti throughout the optimization.

**Acknowledgment.** This work was supported by a grant from the National Institutes of Health (GM) (to A.S.). The Notre Dame Radiation Laboratory is supported by the Office of Basic Energy Sciences of the United States Department of Energy. This is Document No. NDRL-4748 from the Notre Dame Radiation Laboratory.

**Supporting Information Available:** Calculated  $^3J_{\text{COCC}}$  in  $\beta$ -(1  $\rightarrow$  4)-linked disaccharide mimics determined by DFT (data taken from ref 2) (Figure S1); calculated  $^3J_{\text{C2',C4}}$  values by DFT in a model  $\beta$ -(1  $\rightarrow$  4)-linked disaccharide (Figure S2); complete ref 8; Cartesian coordinates for structures **2–7**. This material is available free of charge via the Internet at <http://pubs.acs.org>.

JO702288H

(6) Becke, A. D. *J. Chem. Phys.* **1993**, *98*, 5648–5652.

(7) Hehre, W. J.; Ditchfield, R.; Pople, J. A. *J. Chem. Phys.* **1972**, *56*, 2257–2261.

(8) Frisch, M. J.; *et al.* *Gaussian03*, revision C.02; Gaussian, Inc.: Wallingford, CT, 2004.

(9) Stenutz, R.; Carmichael, I.; Widmalm, G.; Serianni, A. S. *J. Org. Chem.* **2002**, *67*, 949–958.